ELSEVIER

Journal of Photochemistry and Photobiology A: Chemistry 122 (1999) 191–197

Journal of Photochemistry and Photobiology A:Chemistry

Photophysics of photochromic spiroperimidinecyclohexadienone

Vladimir A. Kharlanov*

Institute of Physical and Organic Chemistry, Rostov State University, Stachka str. 104/2, Rostov on Don 344090, Russia

Received 25 January 1999; accepted 4 February 1999

Abstract

Fragment interaction in photochromic spiroperimidinecyclohexadienones **I** was studied by absorption spectroscopy and semiempirical calculations. Absorption spectra of spirans **I** can be presented as an approximate superposition of the spectra for compounds **III** and **IV** modelling the spiran fragments. The weak, long-wavelength absorption band of **I** at ca. 24 600 cm^{-1} is absent in the spectra of model compounds and cannot be attributed to the individual absorption of molecular fragments. The CNDO/S calculation of optical transitions for the spiran structures optimized by AM1 and PM3 has shown that the long-wavelength band is formed by forbidden transition $S_0 \rightarrow S_1$ with mixed $n\pi^*$-CT nature. All other singlet states observed in the spiran spectrum are of the LE nature. The S_2 and S_4 states are localized on the perimidine fragment and the S_3 state is the $\pi\pi^*$ state of the cyclohexadienone fragment. Investigations of all the spirosystems in polar and nonpolar solutions, polymeric films and crystal phase at various temperatures (77–300 K) have shown the absence of fluorescence and phosphorescence for compounds **I**. This phenomenon is explained by the formation of an intermediate for photoconversion of the spiran structure to the quinonimine one.

Keywords: Spiroperimidinecyclohexadienone; Absorption spectra; Spiran structures; Photophysics

1. Introduction

Investigations [1–9] of spiroperimidinecyclohexadienones have shown that spiran structure **I** is converted by photoexcitation to quinonimine structure **II** and this reaction is thermoreversible (Scheme 1). The heteroanalogues of spiroperimidinecyclohexadienone **I** [10–14] undergo similar conversions. Various factors produce substantially different effects on the photoprocess. Intermolecular interactions can inhibit (atmospheric oxygen in polar solvents [1,4,5,7]) or stimulate (nucleophilic agents in polar solvents [7]) the reaction **I** → **II**. However, the role of many important intramolecular factors, as for instance, the interaction of spiran fragments and their electron properties, remains to be clarified. To solve this problem, here, we focus on the spectroscopical study of spiroperimidinecyclohexadienone photophysics as well as on semiempirical calculations of spirans **I** and model compounds **Id, Ill, IVa**, and **IVb** (Scheme 2).

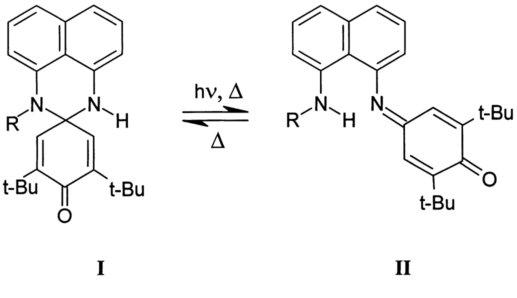

I **II**

R: H (a); CH_3 (b); $CH_2CH(CH_3)_2$ (c);

Scheme 1. Photochromic properties of spiroperimidinecyclohexadienone.

2. Experimental

2.1. Materials

Compounds **I–III** and **IVa** were synthesized, purified, and provided to us by Dr. V. Komissarov [1,4,5]. For the compound **IVb**, literature data were used in the present work.

The solvents were purified by the methods described before [1,4–6]. The absence of admixtures was controlled by the luminescence method.

2.2. Spectroscopy

Absorption spectra were recorded with the spectrophotometer SPECORD M40 (Germany), while fluorescence,

---

*E-mail: photo@ipoc.rnd.runnet.ru

PII: S1010-6030(99)00031-3

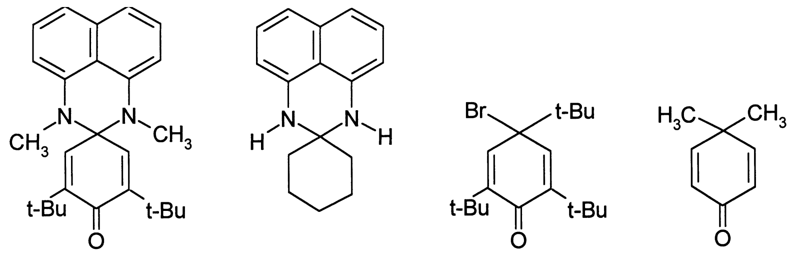

Id **III** **IVa** **IVb**

Scheme 2. Model compounds.

phosphorescence, and luminescence excitation spectra were recorded with spectrofluorometers ELUMIN 2M (Russia) and HITACHI 650–60 (Japan) with correction. Low-temperature measurements (77 K) of luminescence spectra were performed in the optical quartz Dewar vessel.

2.3. Photochemical investigation

In photochemical experiments, solutions of the compounds under investigation were irradiated in quartz cells by a 250 W high-pressure mercury lamp. Discrete spectral lines of exciting light were selected by standard filters.

2.4. Methods of calculations

Ground state calculations were carried out with full geometry optimization using the AM1 [15] and the PM3 [16] programs in the MOPAC 7.0 package [17]. The geometry optimization was performed using Newton algorithm with vibrational analysis of the optimized structure so as to determine stable and transition geometries.

Calculations of absorption transition energies and oscillator strengths were carried out using the CNDO/S method with 50 singly excited configurations and different parameter sets [18–25] for the fully AM1- and PM3-optimized ground state structures.

3. Results and discussion

3.1. Absorption spectra

The data on the absorption spectra of spirans **Ia**–**Id** are presented in Table 1. The spectra of all the compounds are similar and that of **Ia** is presented in Fig. 1(a). As is evident from the comparison of spectra in Fig. 1 and Table 2, an orthogonality of the perimidine and cyclohexadienone fragments in spirans (corroborated by X-ray analysis [4]) enables their absorption spectra to be regarded as an approximate superposition of the corresponding spectra for model compounds **III** and **IVa** or **IVb**.

Table 1
Absorption bands (ν, cm^{-1} (ε, M^{-1} cm^{-1})) of spirans **I** (ethanol, 296 K)

Ia	Ib	Ic	Id
42 800 (53 270)	–	42 720 (52 250)	43 080 (52 650)
38 000 (2870)	38 000 (4380)	38 000 (4780)	–
30 000 (12 020)	30 000 (12 560)	30 000 (12 860)	30 640 (12 470)
28 880 (11 610)	28 880 (12 330)	28 880 (13 090)	29 360 (12 280)
24 480 (1720)	24 480 (1770)	24 320 (1750)	23 920 (1600)

The absorption band with the maxima 30 000 and 28 880 cm^{-1} in the spectrum of the spiran is similar in position, structure, and intensity to the corresponding band of perimidine III, and therefore, can be attributed to the absorption of this fragment (Table 2). The absorption band position for compounds **I** (42 800 cm^{-1}) is the same as for **III** and **IVa**, with the band intensity approximately equal to

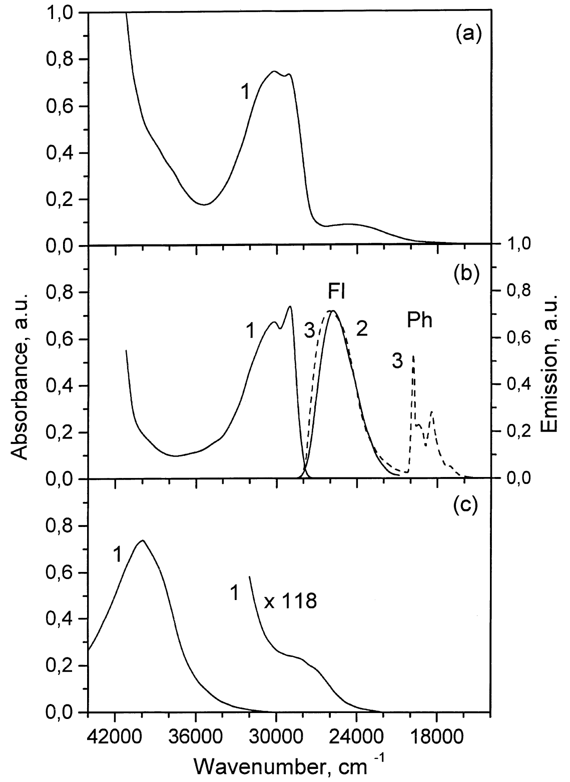

Fig. 1. The absorption spectrum at 295 K (curve 1), and the emission spectra at 295 K (curve 2) and 77 K (curve 3) for (a) spiran **Ia**, (b) perimidine **III**, and (c) cyclohexadienone **IVa**. The data refer to ethanolic solutions of compounds **Ia, III, and IVa**.

Table 2
Spectroscopic data on absorption (ν, cm^{-1}) (ε, M^{-1} cm^{-1}) and luminescence data for compounds **Ia, III**, and **IVb** in ethanol

Spectral data	**III**	**Ia**	**IVb**[a,b] [26]
Absorption bands[c]	42 320 (27 970) – ($\pi\pi^*$)	42 800 (53 270) – ($\pi\pi^*$)	38 500 (24 000) – ($\pi\pi^*$)
	30 000 (11 220) – ($\pi\pi^*$)	30 000 (12 020) – ($\pi\pi^*$)	–
	28 840 (11 520) – ($\pi\pi^*$)	28 880 (11 610) – ($\pi\pi^*$)	–
	–	24 480 (1720) – (nπ^* + CT)	26 800 (68) – (nπ^*)
Fluorescence at 77 K[d]	26 320 (380)	–	–
Fluorescence at 296 K[e]	24 690 (405)	–	–
Phosphorescence at 77 K[f]	19 380 (516)	–	24 920 (401)
	18 870 (530)	–	24 090 (415)
	17 860 (560)	–	23 730 (421)
			23 470 (426)

[a] Absorption in hexane.
[b] Absorption bands of **IVa** are 39 920 cm^{-1} (14 030) and 26 000 cm^{-1} (38) in octane.
[c] Values in parenthesis correspond to extinction coeffecients ε in M^{-1} cm^{-1}.
[def] Values in parenthesis correspond to wavelength in nanometer.

summed intensities for the latter. Thus, the band for **I** is likely to contributed by both fragments.

The weak nπ^* band at ca. 26 000 cm^{-1} of the cyclohexadienone fragment (see Table 2 and Fig. 1(c)) is not detectable in the spiran spectrum as it is shielded by a more intensive band of spiran absorption at ca. 24 300 cm^{-1} which is absent in the spectra of model compounds **III** and **IV**. Consequently, this band cannot be attributed to the individual absorption of molecular fragments and is presumably a result of fragment interaction. Since the perimidine fragment (aromatic amine) and the cyclohexadienone fragment (quinone) represent the electron donor and the acceptor, respectively, [27,28], the band concerned is assumed to arise from a charge transfer transition. To determine unambiguously whether it is the case, and to elucidate the nature of other absorption bands for spirans **I**, the geometry and electron transitions of these compounds were studied by semiempirical computational methods.

3.2. Analysis of the nature of singlet excited states

Our previous study of the spiran geometry by semiempirical methods showed that the spiran could have four stable conformations with the energy distinction between the most and the least stable conformers around 6.0–7.5 kJ/mol (AM1 and PM3) [29]. The fully optimized structure of the more stable conformer of **Ia** is shown in Fig. 2 and its geometrical parameters in comparison with a real structure are presented in Table 3.

The geometry of **Ia** calculated by AM1 and PM3 shows all the peculiarities of the real structure, namely, the spiran fragments are perpendicular to each other and the perimidine fragment is folded along the N11–N13 line, whereas the cyclohexadienone fragment has the boat conformation. The latter is caused by *t*-butyl groups, as is retold later, from the fact that the optimized spiran with cyclohexadienone without the *t*-butyls is planar.

The CNDO/S calculation of optical transitions for the structures optimized by various methods has shown that the long-wavelength transition $S_0 \rightarrow S_1$ is forbidden, and refers to the transfer of the lone electron pair of the oxygen atom from the orbital 65 to the π orbital 72 of the cyclohexadienone fragment and to the π orbital 76 of the perimidine fragment (see Fig. 3 and Table 4). Also, this transition is contributed to significantly by the electron transfer from the orbital 69 of perimidine to the orbital 72 of cyclohexadienone. Thus the $S_0 \rightarrow S_1$ transition is of the mixed nπ^*-CT nature. It gives rise to the long-wavelength absorption band shifted to red and enhanced as compared to an ordinary nπ^* transition. The analogous effect is known for other rigid molecular systems with two decoupled conjugated fragments, one of which is a carbonyl [30,31].

The various methods provided slightly differing optimized geometries for the spiran fragment which was, however, insignificant for the S_1 state nature. For the PM3-

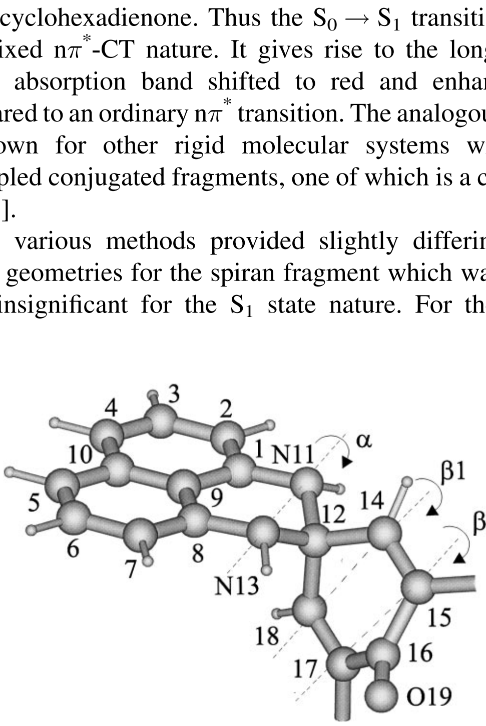

Fig. 2. The structure of spiran **Ia** derived from the PM3 calculation. (*t*-butyl groups are not indicated).

Table 3
The calculated (for spiran **Ia**) and experimentally measured (for spiran **Ib**) values of bond distances and angles for atoms numbered as in Fig. 2

	Calculated by AM1 for **Ia** structure	Calculated by PM3	X-ray structure of **Ib** [4]
Bond distances (Å)			
1–2	1.3928	1.38 06	1.36 9 (3)
2–3	1.4098	1.41 08	1.40 0 (3)
3–4	1.3730	1.36 98	1.36 4 (4)
4–10	1.4211	1.42 03	1.40 2 (3)
5–10	1.4207	1.42 06	1.42 4 (3)
5–6	1.3733	1.36 96	1.34 4 (4)
6–7	1.4094	1.41 10	1.40 0 (4)
7–8	1.3932	1.38 04	1.38 3 (3)
8–9	1.4381	1.42 70	1.41 0 (3)
9–10	1.4123	1.40 75	1.41 3 (3)
1–N11	1.4052	1.43 12	1.38 2 (2)
8–N13	1.4041	1.43 23	1.39 4 (2)
N11–12	1.4814	1.50 27	1.45 8 (2)
N13–12	1.4820	1.50 07	1.48 0 (2)
12–14	1.5343	1.51 53	1.50 6 (2)
14–15	1.3410	1.34 09	1.33 1 (2)
15–16	1.4880	1.49 69	1.48 8 (3)
16–17	1.4911	1.49 99	1.49 8 (3)
17–18	1.3406	1.34 03	1.32 6 (3)
18–12	1.5366	1.51 81	1.49 2 (3)
16–019	1.2354	1.21 50	1.21 9 (3)
Bond angles (°)			
1–N11–12	117.4	116.4	120.2
8–N13–12	117.5	116.4	116.2
N11–12–N13	112.7	109.2	106.8
14–12–18	108.7	109.7	112.0
α	20.9	25.5	41.6
$\beta 1$	16.1	16.1	10.8
$\beta 2$	16.9	21.7	21.3
γ	83.8	92.1	87.8

produced geometry, the charge transfer contribution includes the transfer from the cyclohexadienone to the perimidine fragment (65 → 76) and the reverse one (69 → 72). That is why, the dipole moments of the S_1 and the S_0 state differ slightly (3.12 and 3.05 D, respectively, as shown in Table 4). In contrast, the AM1-produced geometry doesn't give rise to the reverse charge transfer, which results in a large dipole moment difference between the S_1 and the S_0 state (7.58 and 2.70 D).

Table 4
Characteristics of the $S_0 \rightarrow S_1$ transition for spiran **Ia** calculated by CNDO/S (with the geometry optimized by PM3 and AM1)

Characteristic	PM3	AM1
Transition energy, eV	3.84	3.67
Oscillator strength	0.0011	0.0003
Configuration interaction (coefficient)	65 → 72 (−0.7316)	65 → 72 (0.7001)
	65 → 76 (0.3964)	68 → 72 (0.3762)
	69 → 72 (0.3484)	65 → 71 (−0.3686)
	66 → 72 (0.2298)	65 → 77 (0.2664)
	67 → 72 (−0.2269)	65 → 76 (0.2188)
μ ($S_0 \rightarrow S_1$), D	3.05 → 3.12	2.70 → 7.58
Assignment	$n\pi^* + CT$	$n\pi^* + CT$

The S_2 and S_3 states of the spiran **Ia** have the LE nature, with the corresponding transitions localized in the perimidine fragment (see Table 5) in accordance with the analysis of the absorption spectra. The absorption band with the maxima at 30 000 and 28 880 cm^{-1} is likely to arise from both transitions. The next singlet excited state has the CT nature but the transition is not observable in the spectrum due to its small intensity ($f = 0.0051$).

Thus, the following scheme can be presented for the excited states of the spiran, which generalizes the above consideration (see Fig. 4). The S_1 state of the spiran (with the corresponding absorption maximum at 408 nm) results from the $n\pi^*$ state localized on the cyclohexadienone fragment (the lowest lying singlet state of the model compounds **IVa** or **IVb** with the absorption maximum at 373 nm), which is affected by the interaction with the perimidine fragment.

All other singlet states observed in the spiran spectrum are of the LE nature. The S_2 and S_4 states are localized on the perimidine fragment and the S_3 state is the $\pi\pi^*$ state of the cyclohexadienone fragment.

3.3. The luminescence of spiran and model compounds

To determine the triplet states and deactivation paths for excited states of spirans, the luminescence of spirans **I** (Scheme 1) and model compounds (Scheme 2) was investigated.

Investigations of all the spirosystems in polar and non-polar solutions, polymeric films, crystal phase at various

Table 5
Characteristics of the transitions for spiran **Ia** calculated by CNDO/S (with the geometry optimized by PM3[a])

Characteristic	$S_0 \rightarrow S_2$	$S_0 \rightarrow S_3$	$S_0 \rightarrow S_4$
Transition energy, eV	4.01	4.33	4.93
Oscillator strength	0.0338	0.1637	0.0051
Configuration interaction (the relative contribution)	70 → 73 (0.8255)	70 → 71 (−0.9623)	70 → 72 (0.6949)
	68 → 71 (−0.5324)	68 → 73 (−0.2351)	69 → 72 (−0.6233)
			65 → 72 (−0.2293)
μ ($S_0 \rightarrow S_i$), D	3.05 → 3.03	3.05 → 2.92	3.05 → 13.47
Assignment	LE	LE	CT

[a] The transition characteristics for the geometry optimised by AM1 are much the same as in Table 5 and imply the same transition assignments.

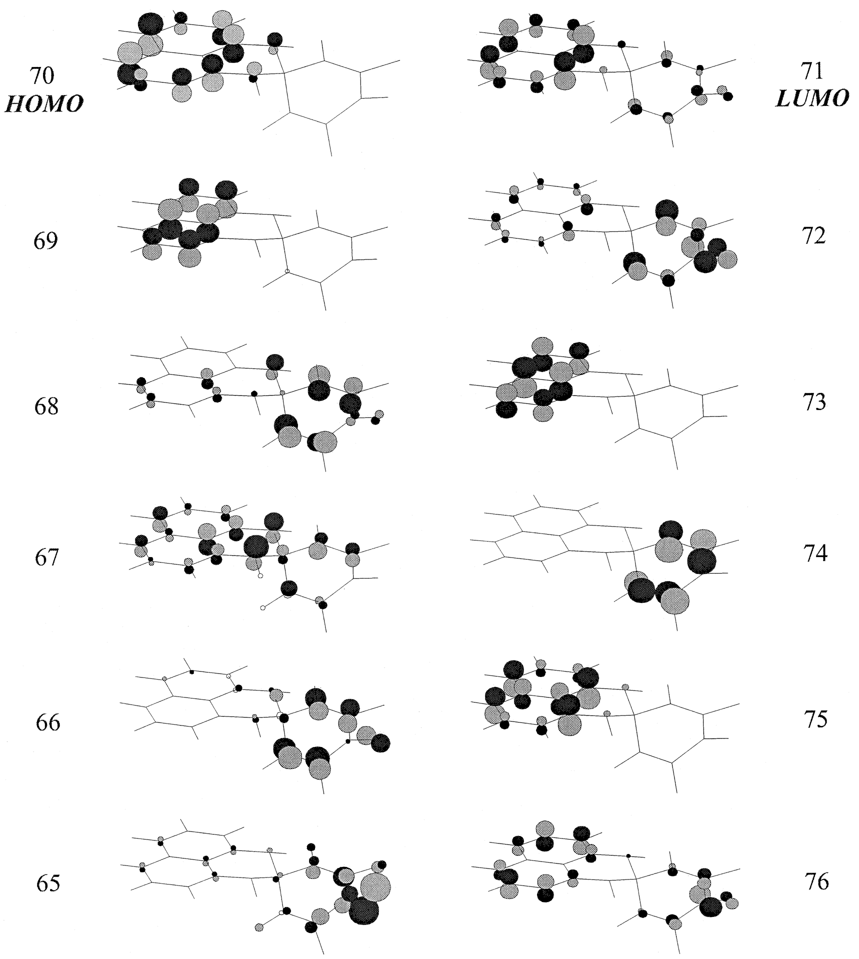

Fig. 3. Unoccupied (on the left) and occupied (on the right) molecular orbitals contributing to the low-lying excited states of **Ia** (from the CNDO/S calculation with the PM3-produced geometry).

temperatures (77–300 K) showed the absence of fluorescence and phosphorescence for compounds **I** (see Table 2). This phenomenon could not have been caused by the immediate photoconversion of the spiran structure **I** to the quinonimine **II** structure. Otherwise luminescence would have been observed for spiran **Id** in which this conversion is impossible in principle.

In contrast to spirans, perimidine **III** displays fluorescence both at room temperature and at 77 K, in the latter case it being shifted to blue by 1630 cm^{-1} (see Table 2 and Fig. 1(b)). This shift is likely to originate from the slowed down orientation relaxation rate for polar solvent molecules [32]. Perimidine also shows phosphorescence with a vibrational structure at 77 K (see Table 2, Fig. 1(b)). The phosphorescence region for **III** (19 380 cm^{-1}) is shifted to longer wavelengths compared to cyclohexadienone (24 920 cm^{-1}) and hence the T_1 state of spiran can be assumed to have the LE nature with the localization on the perimidine fragment. The latter assumption is supported by the results of geometry optimization for spiran performed by various methods (see Table 6). Irrespective of the optimization technique, the CNDO calculation provides the same main configuration

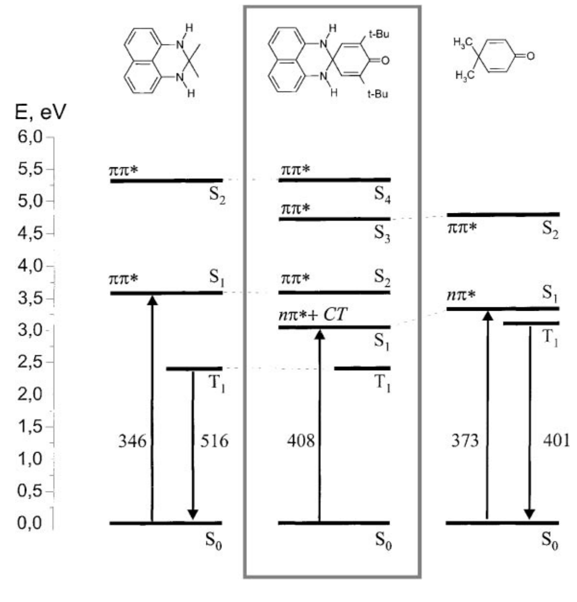

Fig. 4. Formation of excited states of spirans **I** from the perimidine and cyclohexadienone states.

Table 6
Characteristics of the T_1 state for spiran **Ia** calculated by CNDO/S (with the ground-state geometry optimized by PM3 and AM1)

Characteristic	PM3	AM1
State energy, eV	2.33	2.27
S_1–T_1, energy gap, eV	1.23	1.40
Main configuration interaciton	70 → 71	70 → 71
Assignment	LE	LE

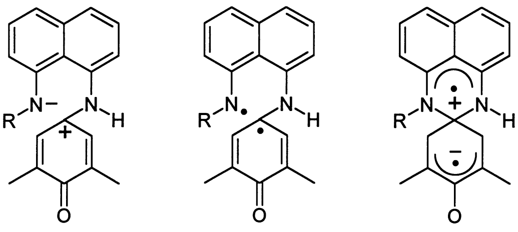

I1 **I2** **I3**

Scheme 3.

for the T_1 state, 70 → 71, with the orbitals localized on the perimidine fragment. It is possible that the triplet state localized on the cyclohexadienone fragment is a rather high lying one (see Fig. 4).

3.4. Photoconversions of spirans

The results obtained in the present study of spiran photophysics also give a deeper insight into the latter's photochemistry. As pointed out, the absence of luminescence suggests that the photoconversion of spiran involves the formation of an intermediate. If it were not the case, the spiran **Id** wherein the quinonimine fragment cannot, in principle, result would exhibit fluorescence or phosphorescence. The plausible electron structures of the intermediate are given in Scheme 3).

Intermediates **I1** and **I2** are formed by heterolytic and homolytic cleavage, respectively, of the N–C(sp^3) bond. Biradicaloid structure **I3** is formed by intramolecular electron transfer into the lowest lying singlet state of spiran classified as an $n\pi^* + \mathrm{CT}$ state. The possibility for the intermediate as well as its electron structure to form can be clarified by an additional ab initio calculation of the excited state for a model spiran.

Also, further investigation is required to determine whether the quinonimine fragment forms via a singlet or a triplet pathway. The method for tackling this problem appears to involve triplet and singlet quenching of the photoreaction of interest.

4. Conclusions

By the comparative analysis of the absorption spectra combined with semiempirical calculations for spirans and model compounds, the nature of the S_1 ($n\pi^*$–CT) and T_1 (LE localized on the perimidine fragment) states was elucidated for all spirans **I**. As shown, the photoconversion of spirans is likely to proceed via the intermediate which is responsible for luminescence quenching in these compounds.

Acknowledgements

We thankfully acknowledge the generous help of Dr. V. Komissarov who provided a number of compounds to us. The present work was financially supported by the Russian Foundation of Fundamental Investigation (RFFI) (Project of RFFI No. 97-03-32017a).

References

[1] V.N. Komissarov, V.A. Kharlanov, L.Yu. Ukhin, V.I. Minkin, Dokl. AN SSSR 301 (1988) 902–905.
[2] V.N. Komissarov, V.A. Kharlanov, L.Yu. Ukhin, Z.S. Morkovnik, V.I. Minkin, M.I. Knyazhansky, Zhurn. Organ. Khim. 26 (1990) 1106–1110.
[3] V.A. Kharlanov, V.N. Komissarov, L.Yu. Ukhin, M.L. Osipova, M.I. Knyazhansky, Zhurn. Organ. Khim. 27 (1991) 1765–1770.
[4] S.M. Aldoshin, M.L. Novozhilova, L.O. Atovmyan, V.N. Komissarov, V.A. Kharlanov, L.Yu. Ukhin, V.I. Minkin, Izvest. AN SSSR, Ser. Khim. (1991) 702–708.
[5] S.M. Aldoshin, M.L. Novozhilova, L.O. Atovmyan, V.N. Komissarov, V.A. Kharlanov, L.Yu. Ukhin, V.I. Minkin, Izvest. AN SSSR, Ser. Khim. (1991) 1121–1129.
[6] S.M. Aldoshin, M.L. Novozhilova, L.O. Atovmyan, V.N. Komissarov, L.Yu. Ukhin, V.A. Kharlanov, Izvest. AN SSSR, Ser. Khim. (1991) 1802–1807.
[7] V.A. Kharlanov, M.I. Knyazhansky, V.E. Kuznetzov, Zhurn. Organ. Khim. 28 (1992) 1093–1095.
[8] V.I. Minkin, V.N. Komissarov, V.A. Kharlanov, in: J.C. Crono, R. Guglielmetti (Eds.), Organic Photochromic and Thermochromic Compounds, vol. 1, Main Photochromic Families, Ch 8, Plenum Press, New York, 1998.
[9] V.I. Minkin, V.N. Komissarov, Mol. Cryst. Liq. Cryst. 297 (1997) 205–212.
[10] E.N. Postupnaja, V.N. Komissarov, V.A. Kharlanov, Zhurn. Organ. Khim. 29 (1993) 1915–1916.
[11] V.N. Komissarov, E.N. Gruzdeva, V.A. Kharlanov, V.A. Kogan, V.I. Minkin, Zhurn. Organ. Khim. 29 (1993) 2030–2034.
[12] V.N. Komissarov, E.N. Gruzdeva, V.A. Kharlanov, L.P. Olekhnovich, G.S. Borodkin, V.I. Khrustalev, S.V. Lindeman, Yu.T. Struchkov, V.A. Kogan, V.I. Minkin, Izvest. RAN, Ser. Khim. 11 (1997) 2028–2033.
[13] V.N. Komissarov, E.N. Gruzdeva, V.A. Kharlanov, L.P. Olekhnovich, G.S. Borodkin, V.I. Khrustalev, S.V. Lindeman, Yu.T. Struchkov, V.A. Kogan, V.I. Minkin, Russ. Chem. Bull. 46 (1997) 1924–1930.
[14] A.V. Metelitsa, V.N. Komissarov, M.I. Knyazhansky, V.I. Minkin, Mol. Cryst. Liq. Cryst. 297 (1997) 219–226.
[15] M.J.S. Dewar, E.G. Zoebisch, E.F. Healy, J.J.P. Stewart, J. Am. Chem. Soc. 107 (1985) 3202.
[16] J.J.P. Stewart, J. Comp. Chem. 10 (1989) 209.
[17] J.J.P. Stewart, MOPAC 7.0: Semiempirical Molecular Orbital Program, Program No. 455, Quantum Chemistry Program Exchange (QCPE), Indiana University, Bloomington, IN 47405, USA.
[18] J. Del Bene, H.H. Jaffe, J. Phys. Chem. 48 (1968) 1807.
[19] J. Del Bene, H.H. Jaffe, J. Phys. Chem. 48 (1968) 4050.

[20] J. Del Bene, H.H. Jaffe, J. Phys. Chem. 49 (1968) 1221.
[21] J. Del Bene, H.H. Jaffe, J. Phys. Chem. 50 (1969) 1126.
[22] H.M. Chang, H.H. Jaffe, C.A. Masmanidis, J. Chem. Phys. 79 (1975) 1109–1118.
[23] J. Del Bene, J. Am. Chem. Soc. 95 (1973) 6517.
[24] J. Del Bene, J. Chem. Phys. 62 (1975) 666.
[25] J. Del Bene, J. Chem. Phys. 62 (1975) 1961.
[26] H.E. Zimmerman, R.W. Binkley, I.J. MeCullogh, G.A. Zimmerman, J. Am. Chem. Soc. 89 (1967) 6589.
[27] L. Eberson, Electron Transfer Reactions in Organic Chemistry, Springer, Berlin, 1987.
[28] S.L. Murov, I. Carmichael, G.L. Hug, Handbook of Photochemistry, 2nd ed., Marcel Dekker, New York, Basel, Hong Kong, 1993, pp. 261–276.
[29] V.A. Kharlanov, Zh. Organ. Khim., in press.
[30] E.S. Stern, C.J. Timmons, Electronic Absorption Spectroscopy in Organic Chemistry, Ch 3, Edward Arnold, London, UK, 1979.
[31] H. Labhart, G. Wagniere, Helv. Chim. Acta 42 (1959) 2219.
[32] N.G. Bakhshiev, Spectroscopy of Intermolecular Interactions, Nauka, Leningrad, 1972.